

THE IMPACT OF GALAXY GEOMETRY AND MASS EVOLUTION ON THE SURVIVAL OF STAR CLUSTERS

JUAN P. MADRID, JARROD R. HURLEY, MARIE MARTIG

Center for Astrophysics and Supercomputing, Swinburne University of Technology, Hawthorn, VIC 3122, Australia
ApJ accepted

ABSTRACT

Direct N -body simulations of globular clusters in a realistic Milky Way-like potential are carried out using the code NBODY6 to determine the impact of the host galaxy disk mass and geometry on the survival of star clusters. A relationship between disk mass and star cluster dissolution timescale is derived. These N -body models show that doubling the mass of the disk from $5 \times 10^{10} M_{\odot}$ to $10 \times 10^{10} M_{\odot}$ halves the dissolution time of a satellite star cluster orbiting the host galaxy at 6 kpc from the galactic center. Different geometries in a disk of identical mass can determine either the survival or dissolution of a star cluster orbiting within the inner 6 kpc of the galactic center. Furthermore, disk geometry has measurable effects on the mass loss of star clusters up to 15 kpc from the galactic center. N -body simulations performed with a fine output time step show that at each disk crossing the outer layers of star clusters experience an increase in velocity dispersion of $\sim 5\%$ of the average velocity dispersion in the outer section of star clusters. This leads to an enhancement of mass-loss – a clearly discernable effect of disk shocking. By running models with different inclinations we determine that star clusters with an orbit perpendicular to the Galactic plane have larger mass loss rates than both clusters evolving in the Galactic plane or in an inclined orbit.

Subject headings: Galaxy: star clusters: general: galaxies: star clusters - galaxies: dwarf - galaxies: stars: evolution

1. INTRODUCTION

In the current paradigm of galaxy formation smaller structures merge into larger ones from the Big Bang up to the present day (White & Rees 1978). Galaxies grow through two main processes: the hierarchical merging with smaller galaxies and the accretion of fresh gas fuelling new star formation. These different mechanisms contribute to the growth of the disk, bulge and halo.

As the first significant stellar structures to form, globular clusters witness the entire evolution of their host galaxy as satellite systems. Indeed, globular clusters are believed to follow galaxies during galaxy mergers and close encounters (e.g. West et al. 2004). The gravitational potential of their host galaxy has a direct influence on the survival of globular clusters: they lose stars through tidal stripping and disk shocking. In turn, these lost stars contribute to the build-up of the galaxy's stellar halo. The evolution of host galaxy and globular clusters are clearly connected.

The aim of this work is to derive, using numerical simulations, the importance of the host galaxy disk mass and size on the evolution and survival of star clusters. How are satellite stellar systems affected by disks and bulges of changing mass and with different geometries? And reciprocally, how do satellite stellar systems contribute, through their dissolution, to the formation of the halo of the host galaxy?

D'Onghia et al. (2010) show that halo and disk shocking efficiently deplete the satellite population of dark matter halos within 30 kpc of the Milky Way center. The results of that study cannot be directly applied to globular clusters because of their much higher densities compared to dark matter halos.

In their important paper, Gnedin & Ostriker (1997) model the dynamical evolution of the Galactic globular cluster system using a Fokker-Planck code. These au-

thors build on earlier analytical work by Aguilar, Hut & Ostriker (1988) and Kundic & Ostriker (1995) among others. Gnedin & Ostriker (1997) give analytical expressions to estimate the impact of disk shocking and also call for numerical simulations to be carried out.

With the recent progress in computational capacity, large N -body simulations can now be carried out in order to determine the physical mechanisms that govern the dynamical evolution of globular clusters in a galactic potential. Recently, Renaud & Gieles (2013) found that after a merger event of the host galaxy the mass loss rate of a satellite star cluster increases. Interestingly, Renaud & Gieles (2013) also find that even if the tidal forces reach a maximum during the merger itself they are too short-lived to have a significant impact on the long term survival of star clusters.

Previous work on the mass loss of star clusters focused on internal dynamical effects and stellar evolution. Vesperini & Heggie (1997) carried out numerical simulations of star clusters and determined their mass loss rates through a Hubble time. Baumgardt & Makino (2003) established an analytical dissolution time scale for star clusters and showed that one third of the cluster mass is lost due to stellar evolution alone. A recent review by of recent N -body studies can be found in Portegies Zwart et al. (2010).

The approach in our work is purely numerical and different in nature to Gnedin & Ostriker (1997) given that no assumptions or explicit expressions to treat the impact of the disk are used. N -body models of star clusters were run where the properties of the star cluster remain identical but the mass and geometry of the galactic disk change. The effect of the disk on the star cluster is computed as a part of the numerical calculations of the gravitational force experienced by each star.

The above is carried out with the code NBODY6 used

for the study of the dynamics of star clusters through N -body simulations. **NBODY6** now includes a detailed model of the host galaxy where star clusters evolve as satellites (Aarseth 2003). The current set-up of **NBODY6** includes the tools to model a Milky-Way type galaxy with three distinct components: disk, bulge, and halo. The gravitational force for each star of the cluster is computed at each time step by taking into account the effect of all other stars, and of the disk, bulge, and halo. We make use of this new capacity of **NBODY6** to run several models of star clusters where the mass and physical size of the disk are different between models.

Throughout this work, a Hubble time of 13.5 Gyr is adopted, in agreement with the results of the Wilkinson Microwave Anisotropy Probe (Spergel et al. 2003).

2. MODELS SET-UP

In the current framework of **NBODY6** the different components of the galactic model are static in time. Indeed the mass of the disk is assumed to be constant over time. In **NBODY6** the disk component of the galaxy is modeled following the prescriptions of Miyamoto and Nagai (1975):

$$\Phi(r, z) = \frac{GM_{DISK}}{\sqrt{r^2 + [a + \sqrt{(z^2 + b^2)}]^2}}. \quad (1)$$

where G is the gravitational constant and M_{DISK} is the mass of the disk. The geometry of the disk can be easily modified by changing the parameters a (scale length) and b (scale height). Different values adopted in previous work for these two parameters and the disk mass are given in Table 1. While different values of these scale parameters are explored in this work, the most often assumed values are $a = 4$ kpc and $b = 0.5$ kpc. Also, a commonly used value for the mass of the bulge is $M_{BULGE} = 1.5 \times 10^{10} M_{\odot}$ (Xue et al. 2008) which we model as a point mass. We model the galactic halo as a logarithmic potential that gives the entire galaxy a rotational velocity of 220 km/s at 8.5 kpc from the galactic center (Aarseth 2003).

The initial set-up of the simulated star clusters is analogous to the simulations presented in Madrid et al. (2012). Briefly, the star clusters start with $N=100\,000$ stars, an initial mass of $6.4 \times 10^4 M_{\odot}$, a half-mass radius of 6.2 pc, and a spatial distribution that assumes a Plummer sphere (Plummer 1911). The initial mass function (IMF) of the simulated star clusters is the one defined by Kroupa (2001), which extends the range given previously by Kroupa et al. (1993). This IMF defines a distribution of stellar masses using the quantity $\xi(m)dm$ which is the number of stars between the masses m and $m+dm$. The explicit expression for $\xi(m)$ is the following broken power law:

$$\xi(m) \propto m^{-\alpha_i}, \quad (2)$$

where $\alpha_1 = 1.3$ for $0.08 \leq m/M_{\odot} < 0.5$ and $\alpha_2 = 2.3$ for $0.5 \leq m/M_{\odot}$. The lightest star in our simulation has a mass of $0.1 M_{\odot}$ while the heaviest has a mass of $50 M_{\odot}$. In addition, all simulations have 5000 primordial binaries, that is 5% of the total number of stars.

Models are run at 6 kpc from the galactic center, unless otherwise stated. At this distance, $R_{GC} = 6$ kpc,

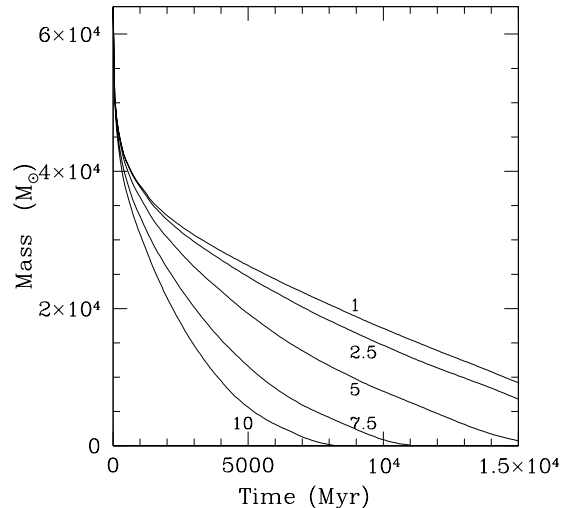


FIG. 1.— Total mass of simulated star clusters vs. time for models with disks of different masses. The labels give the mass of the disk in units of $10^{10} M_{\odot}$, the lightest disk being $1 \times 10^{10} M_{\odot}$. Heavier disk masses enhance mass loss rates and accelerate the dissolution of star clusters.

star clusters are free from bulge shocking while the effect of disk shocking is still strong within the configuration described above. With a few clearly identified exceptions simulated star clusters follow a circular orbit with an initial inclination of $\theta = 22.5$ degrees with respect to the galaxy disk. This inclination gives the star cluster an orbit that is neither planar nor perpendicular to the disk. With this inclination the star cluster has a maximum height of $Z_{MAX} = 2$ kpc comparable with the thick disk. In cartesian coordinates the plane of the disk is in the (x, y) plane.

Similarly to Madrid et al. (2012), stars are removed from the simulation when they have positive energy and when the distance from the center of the cluster is at least two tidal radii. The tidal radius is defined as it was in Madrid et al. (2012), that is following the formula of Küpper et al. (2010):

$$r_t \simeq \left(\frac{GM_C}{2\Omega^2} \right)^{1/3} \quad (3)$$

where Ω is the angular velocity of the cluster around the galaxy, M_C is the mass of the cluster, and G is the gravitational constant. We define an escape radius beyond which stars are no longer part of the simulation. This escape radius scales with the tidal radius over the time evolution of the cluster. The escape radius is at least two times the length of the tidal radius.

The version of **NBODY6** in use through this work is optimized to run on Graphic Processing Units (GPUs). All the models are performed on the GPU Supercomputer for Theoretical Astrophysical Research (gSTAR) hosted at Swinburne University. Each model is computed on one NVIDIA Tesla C2070 GPU in combination with six processing cores on the host node. The approximate computer time to carry out one model of $N=100,000$ stars is three weeks.

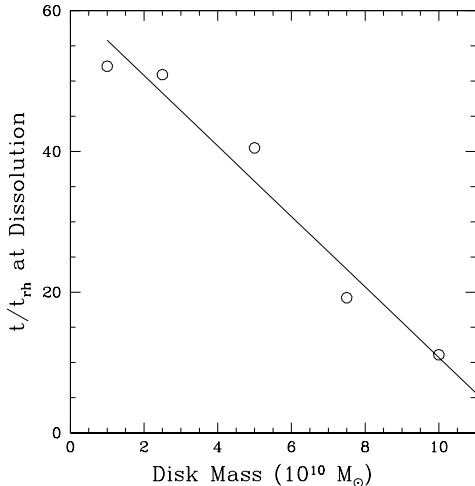


FIG. 2.— Dissolution time/relaxation time (t/t_{rh}) vs. disk mass for star clusters orbiting at 6 kpc from the galactic center. t/t_{rh} is computed when the star cluster has only 10% of its initial mass left. A heavier disk shortens the number of relaxations a star cluster undergoes before dissolution.

3. A HEAVIER OR LIGHTER DISK

Independent models of globular clusters are run with different masses for the host galaxy disk. The mass of the disk is made to vary between $1 \times 10^{10} M_{\odot}$ and $10 \times 10^{10} M_{\odot}$ by incremental steps. The first step is of $1.5 \times 10^{10} M_{\odot}$ while subsequent steps are of $2.5 \times 10^{10} M_{\odot}$. This range of values covers the different masses that a disk has during its evolution according to galaxy formation theory (e.g. Leitner 2012). These disk masses are also consistent with values published in the literature and shown in Table 1. This series of models are run at the same galactocentric distance of 6 kpc, and with the same properties, the only parameter that changes in the simulations is the disk mass. The geometry of the disk is kept constant with $a = 4$ kpc and $b = 0.5$ kpc.

The total mass of simulated star clusters vs. time in simulations with different disk masses is plotted in Figure 1. A natural result of these simulations is that a more massive disk enhances the mass loss rate of an orbiting star cluster owing to a stronger tidal field. An enhanced mass loss rate implies a shortened dissolution time. The star cluster that orbits a “light” disk with a mass of $1 \times 10^{10} M_{\odot}$ has a remaining mass of $1.2 \times 10^4 M_{\odot}$, or 19% of its initial mass, after a Hubble time of evolution. On the other extreme, a star cluster that evolves within a “heavy” disk with a mass of $10 \times 10^{10} M_{\odot}$ is completely dissolved after 8.2 Gyr of evolution. As expected, disks with masses between these two examples define intermediate regimes of mass loss, as shown in Figure 1.

By introducing the half-mass relaxation time t_{rh} , also computed by NBODY6, we can derive a simple relation between the number of relaxations a star cluster undergoes before dissolution and the mass of the disk. The half-mass relaxation time is given by

$$t_{rh} = \frac{0.14N}{\ln \Lambda} \sqrt{\frac{r_{hm}^3}{GM}}, \quad (4)$$

TABLE 1
PUBLISHED VALUES FOR MASS AND STRUCTURAL PARAMETERS OF THE GALACTIC DISK

Reference	Disk Mass (M_{\odot})	a (kpc)	b (kpc)
Bullock & Johnston (2005)	$1.0 \times 10^{11} M_{\odot}$	6.5	0.26
Gómez et al. (2010)	$7.5 \times 10^{10} M_{\odot}$	5.4	0.30
Paczynski (1990)	$8.1 \times 10^{10} M_{\odot}$	3.7	0.20
Peñarrubia et al. (2010)	$7.5 \times 10^{10} M_{\odot}$	3.5	0.3
Read et al. (2006)	$5.0 \times 10^{10} M_{\odot}$	4.0	0.50

NOTE. — This table gives published values for the mass and structural parameters of the disk for Milky-Way type galaxies. The values of a and b correspond to the disk scale length and disk scale height.

where $\Lambda = 0.4N$ is the argument of the Coulomb logarithm, N is the number of stars, and r_{hm} the half-mass radius, (Spitzer & Hart 1971; Binney & Tremaine 1987). Figure 2 shows the number of relaxation times (t/t_{rh}) vs. mass of the disk at the time when the cluster has only 10% of its initial mass left. This quantity ($10\% M_0$) is preferred over the time it takes for the cluster to completely dissolve since numerical simulations become noisy for low N owing to small number statistics. The best fitting linear relation between dissolution time, relaxation time and disk mass is plotted in Figure 2 and is given by

$$t/t_{rh} = -5 \times \frac{M_{DISK}}{10^{10} M_{\odot}} + 61. \quad (5)$$

We find that doubling the mass of the disk from $5 \times 10^{10} M_{\odot}$ to $10 \times 10^{10} M_{\odot}$ leads to the dissolution of the star cluster in half the time.

4. DISK GEOMETRY

The current set-up of NBODY6, based on the formula of Miyamoto and Nagai (1975), allows the geometry of the disk to be modified by changing the values of the parameters a and b of Eq. 1. Table 1 shows that the mass and structural parameters of the Galactic disk take a range of values in different studies. Eighteen models of star clusters where the disk has different scale parameters were carried out in order to evaluate the impact of disk geometry on the survival and evolution of star clusters. Selected parameters of models executed for this section are listed in Table 2.

Three disk models are considered where the concentration of the disk mass density profile varies from a disk mass highly concentrated towards the center of the galaxy to a disk mass with an extended mass profile. Values for the disk scale parameters are $a = 0.4$ kpc and $b = 0.5$ kpc for the first set of models (models 1 through 6 in Table 2). By running models with $a = 0.4$ kpc and $b = 0.5$ kpc the shape of the disk changes to a more centrally concentrated one similar to a prolate bulge, as the value of the scale length parameter a is ten times smaller than the standard value used in the second set of models. The second set of models (labels 10 and 13 to 17 in Table 2) have disk parameters $a = 4.0$ kpc and $b = 0.5$ kpc. A third set of models was carried out with a “flattened” or more extended disk where the scale parameters are $a = 8$ kpc and $b = 0.5$ kpc (models 18 to 23 in Table 2). Altogether, the evolution of 1.9 million stars was simulated for this section.

The disk density profiles of the three different disk geometries are represented in Figure 3. The disk model with the Miyamoto and Nagai scale parameters $a = 0.4$ kpc and $b = 0.5$ kpc is represented on the top panel. In this model, the mass of the disk is highly concentrated towards the center of the galaxy with a very steep fall off: the mid-plane disk density drops from $3.5 \times 10^9 \text{ M}_\odot/\text{kpc}^3$ at $R_{GC} = 1$ kpc to $1 \times 10^7 \text{ M}_\odot/\text{kpc}^3$ at $R_{GC} = 7$ kpc.

For each disk profile we study the evolution of an identical star cluster at six different radii from the galactic center. Models were executed at $R_{GC} = 4, 6, 8, 10, 12.5$, and 15 kpc from the galactic center. In Figure 3, circles with sizes proportional to the masses of the simulated star clusters after 10 Gyr of evolution are drawn at their respective orbital distances. The percentage of the initial star cluster mass remaining after 10 Gyr is also given in Figure 3.

Several simulated clusters do not survive to 10 Gyr, let alone up to a Hubble time. For the first set of models, with a very concentrated disk, the simulated star cluster evolving at 4 kpc from the center of the galaxy is totally dissolved at a record time of only 334 Myr. The simulated star cluster at an orbit of 6 kpc has a remaining mass of only $\sim 870 \text{ M}_\odot$ at 10 Gyr, just $\sim 1\%$ of its initial mass. At 8 kpc from the galactic center the modelled star cluster has 28% of its initial mass after 10 Gyr of evolution.

The middle panel of Figure 3 shows the disk density profile for a disk model with $a = 4$ kpc and $b = 0.5$ kpc, i.e. the same geometry as the models of Section 3. In this second set of models, the star cluster orbiting at 4 kpc is also completely dissolved before 10 Gyr.

The star cluster orbiting at 6 kpc in this more extended disk model (middle panel) has a mass of 7972.8 M_\odot after 10 Gyr of evolution, nine times the mass of the star cluster retained in a centrally peaked disk model. Clusters on orbits of 8 kpc in both models have virtually the same mass, i.e. only 1% difference, after 10 Gyr of evolution. Similarly, for models at $R_{GC} = 10$ kpc and beyond their mass difference is clearly measurable but on the order of 3% for clusters at $R_{GC} = 10$ and 12.5 kpc and 2% for clusters at $R_{GC} = 15$ kpc.

A third set of models, with a more extended disk, was also studied. These models are represented in the bottom panel of Figure 3. With this disk geometry, that is $a = 8$ kpc and $b = 0.5$ kpc, the mass of the disk is more spread out and the additive tidal effects of bulge and disk are not strong enough to completely disrupt the star cluster evolving at $R_{GC} = 4$ kpc. This innermost star cluster survives 10 Gyr of evolution with 8% of its initial mass.

The models presented above show that disk geometry has a clear impact on the globular cluster mass function. This impact is more evident in the inner regions of the galaxy where a centrally concentrated disk (upper panel of Figure 3) adds to the tidal effects of the bulge and enhances the destruction rate of globular clusters within 6 kpc of the galactic center. At $R_{GC} = 8$ kpc there is a switch or transition in the tidal effects following the different disk geometries. Star clusters at $R_{GC} = 10$ kpc and beyond have more mass on the first set of models with the centrally concentrated disk than on the second and third set of models with more extended disks. The tidal effects of the disk are still clearly measurable out to

$R_{GC} = 15$ kpc but are small in intensity, of the order of 3 to 5% of the initial mass.

During 10 Gyr of evolution most of the mass of star clusters within $R_{GC} = 6$ kpc will be transferred to the host galaxy. Mass transfer from globular clusters to the host galaxy in the form of stellar tidal tails has been well documented observationally in Galactic globular clusters and modelled by Küpper et al. (2010). For instance, Odenkirchen et al. (2001) described the presence of two tidal tails emerging from Palomar 5 using SDSS data. After dissolution, the stars that formed the star cluster become part of the host galaxy stellar population.

5. HEATING AND COOLING DURING DISK CROSSINGS

Gnedin & Ostriker (1997) describe the effect of disk shocking as a shock or impulse of extra energy given to each star in the cluster as it crosses the disk (see also Spitzer 1958; Gnedin & Ostriker 1999). Stars close to the tidal boundary can be lost during disk crossing events given that this extra energy allows them to escape from the star cluster. This section presents a close-up of the mass-loss and velocity dispersion of star clusters at each disk crossing.

A simulation with output given at more frequent intervals (every 1 Myr) was carried out to sample in detail the effects of a single disk crossing on a star cluster. The simulated star cluster is placed at 6 kpc from the galactic center with disk scale parameters of $a = 4$ kpc and $b = 0.5$ kpc, an initial orbital inclination of $\theta = 22.5$ degrees and an orbital period of ~ 150 Myr. The height of the star cluster above the plane of the disk and the internal velocity dispersion are represented in Figure 4. The internal velocity dispersion shown in Figure 4 corresponds to the velocity dispersion of the outer 50% of the mass of the cluster, this is the section of the star cluster where individual stars experience the greatest changes in energy during each disk crossing. The velocity dispersion depicted in Figure 4 has been offset from an average level of ~ 2 km/s. For comparison, the average internal velocity dispersion of the entire star cluster is ~ 3 km/s after 3 Gyr of evolution. The maximum height reached by a star cluster is 2 kpc from the plane of the disk.

A periodic impulse given to the velocity dispersion of the outer layers of the star cluster at each disk crossing is evident in Figure 4. The amplitude of this impulse, measured from an average level before disk crossing, is of 0.11 km/s. This increase is 5.2% in the average velocity dispersion of the stars that make up the outer 50% of the star cluster mass. There is a time delay of ~ 7 Myr between the star cluster crossing the equatorial plane of the disk (i.e. $z=0$) and the peak of the impulse in velocity dispersion. This time delay is of the same order of magnitude as the crossing time that is in this case $t_{cross} \sim 2$ Myr. Following its peak the velocity dispersion of the star cluster experiences a reduction of ~ 0.14 km/s on average. Gnedin et al. (1999) mention a “refrigeration effect” or slight reduction in the energy dispersion of a star cluster following a disk shock. Figure 4 shows that at every disk crossing an increase is followed systematically by a decrease in velocity dispersion.

The same velocity dispersion discussed above and the mass of the cluster outside its tidal radius (M_{out}) are plotted in Figure 5. The mass outside the tidal radius M_{out} plotted in Figure 5 corresponds to the mass be-

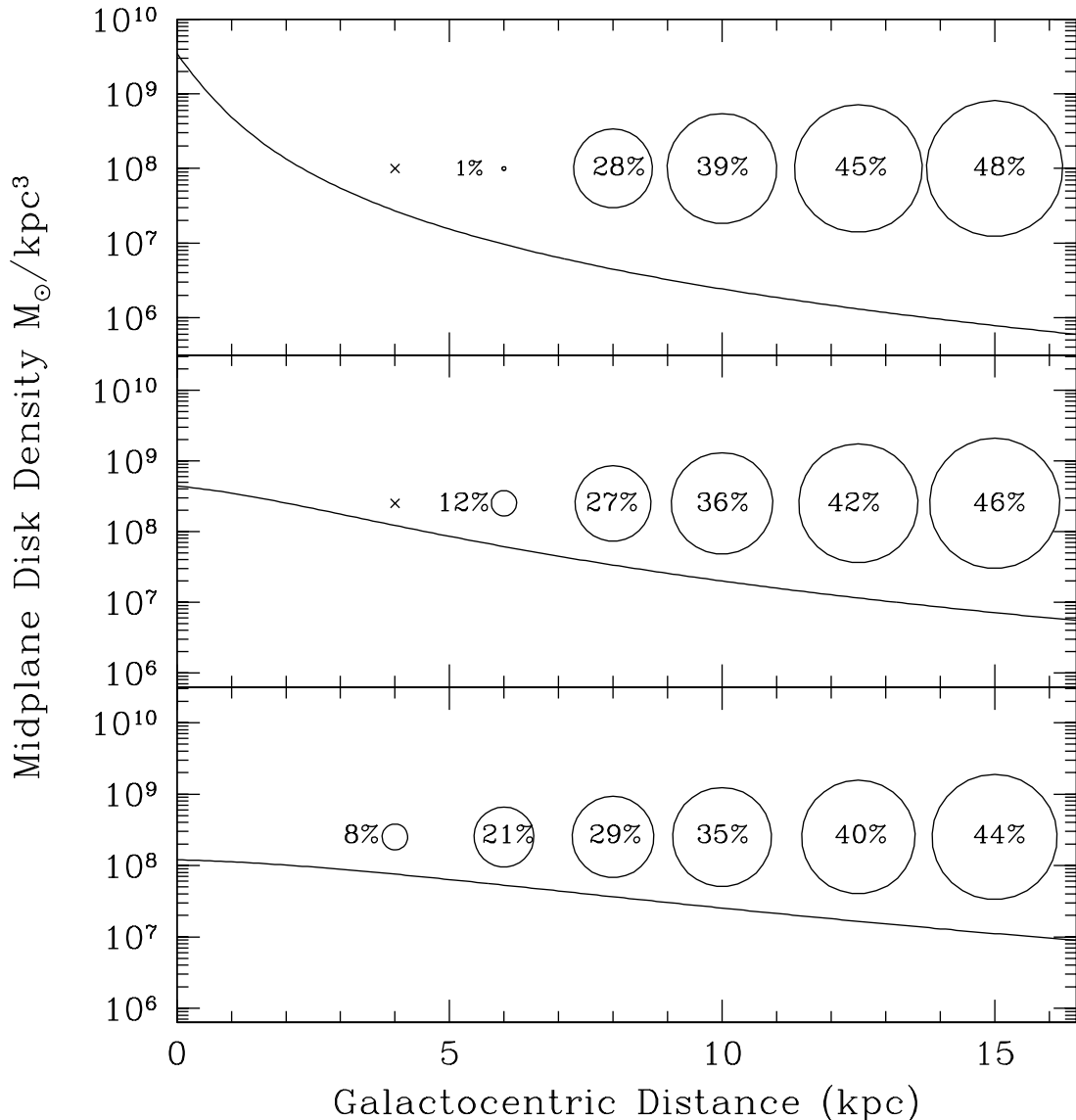


FIG. 3.— Effect of a different disk geometry on orbiting star clusters. The mass density profiles, at the midplane ($z = 0$), for three different disk geometries are plotted as a solid line in each panel. The size of the circles symbolizes the mass remaining in a star cluster after 10 Gyr of evolution. The percentage of the initial mass left is also given for all models. Star clusters are represented at their respective galactocentric distances. *Upper panel:* A galaxy disk with its mass concentrated at the center of the galaxy with scale length parameters of $a=0.4$ kpc and $b=0.5$ kpc. *Middle panel:* Galaxy disk with commonly used parameters $a=4$ kpc and $b=0.5$ kpc. *Lower panel:* A more extended galaxy disk, $a=8$ kpc and $b=0.5$ kpc.

tween the tidal radius and the escape radius. The escape radius is at least twice the length of the tidal radius, as defined in section 2 and in Madrid et al. (2012).

Figure 5 shows that at each disk crossing ($z=0$) the mass outside the tidal radius reaches a minimum, reflecting the strength of the tidal field felt by the star cluster. Over the ten disk crossings represented in Figures 4 the star cluster loses $\sim 2600 M_\odot$, that is on average $260 M_\odot$ per disk crossing. After the star cluster passes the disk its velocity dispersion decreases and the mass outside the tidal radius increases as this region of the cluster fills up due to a weaker tidal field. M_{out} reaches a maximum when the star cluster is at the furthest distance from the disk.

The stars that make up the mass outside the tidal radius come from within the tidal radius as shown in Figure 5: the mass inside the tidal radius decreases when

the mass outside the tidal radius increases. For the time lapsed during the disk crossings represented in Figures 4 and 5, the tidal radius can be considered to be constant. Over longer time scales the tidal radius is a dynamic quantity by virtue of Equation 3.

An elementary estimate for the mass loss during a disk crossing can be derived using the data presented above and previous theoretical work. The energy change for stars in a star cluster is $\Delta E \sim (\Delta V)^2$ (Gnedin & Ostriker 1997) and using the virial theorem $E \propto M^2$ we write that $dM/M \sim dV/V$. Using the simulations above we can give a numerical value to the expression $dM/M \sim dV/V$. The velocity increase in the outer regions of the star cluster has a numerical value of $dV/V \sim 0.1/2.0 = 0.05$ (see Fig. 5, top panel.) The change of mass can also be determined from the simulations, at 3 Gyr, $dM/M = 299/26125 \sim 0.01$. We find

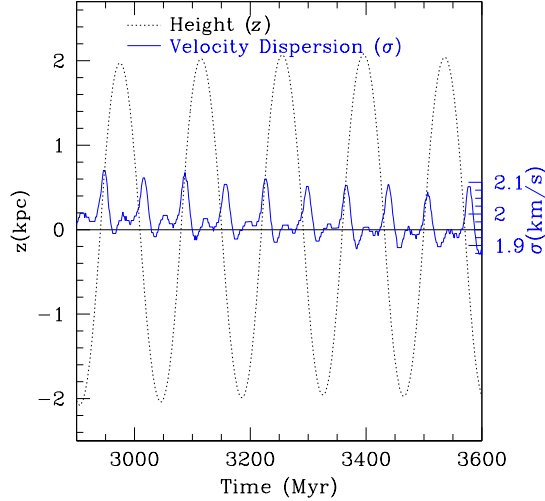


FIG. 4.— Star cluster height above the plane of the disk and velocity dispersion of stars in the outer 50% of the star cluster mass. At each disk crossing the outer layers of the star cluster experience an increase in their internal velocity dispersion. Both height and velocity dispersion have been scaled for display purposes. The average velocity dispersion decreases slightly over the time plotted in Figure 4. The maximum height in the orbit of the star cluster is 2 kpc above the plane of the disk.

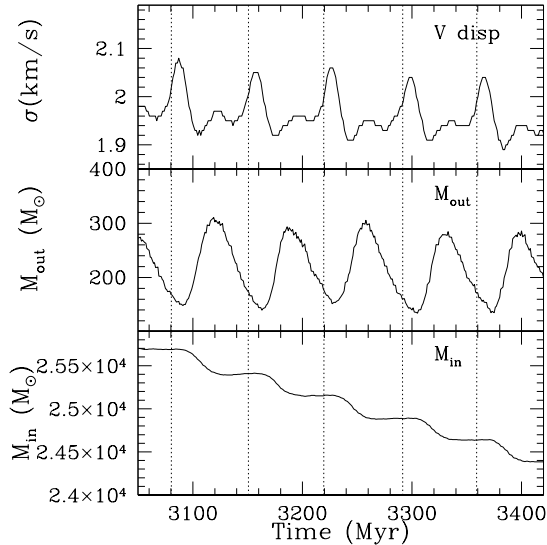


FIG. 5.— *Upper panel:* Velocity dispersion of stars in the outer 50% of the star cluster. *Medium panel:* Mass of the cluster outside the tidal radius (M_{out}). *Lower panel:* Mass inside the tidal radius (M_{in}). The vertical dotted lines mark the crossing of the plane of the disk ($z = 0$). During these five disk crossing the tidal radius can be considered to be constant. The stars that make up the mass outside the tidal radius originate from within the tidal radius.

thus $dM/M \sim 0.2dV/V$, that is, the change of mass is proportional to roughly 20% of the velocity dispersion change induced by a disk crossing.

6. ORBITAL INCLINATION

For a cluster on an inclined orbit the passage through the disk implies an enhanced, or impulsive, gravitational force owing to the proximity of the mass that constitutes the disk, as shown in the previous section. Is the tran-

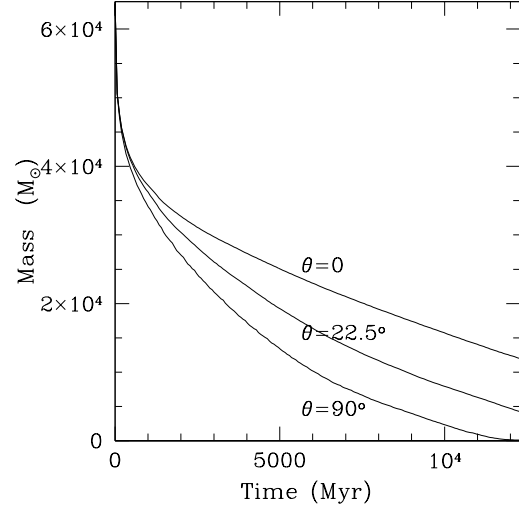


FIG. 6.— Star cluster mass vs. time for three clusters with different orbital inclination. Three inclinations are shown here: a star cluster orbiting in the plane of the disk $\theta = 0$, with a “standard” orbit $\theta = 22.5^\circ$, and perpendicular to the disk $\theta = 90^\circ$.

sient nature of the energy shift that stars receive during disk passages more important than a high but constant tidal field? In order to properly disentangle the tidal effects and those of disk shocking, two simulations with different orbital inclination were carried out. One simulated star cluster orbits the galaxy in the plane of the disk, that is, all its initial velocity is in the y direction $V = V_y$, ($\theta = 0$). A second simulation, with the same characteristics of the previous simulation, evolves in an orbit perpendicular to the disk ($\theta = 90^\circ$), in this case, $V = V_z$. Both simulations evolve at a galactocentric distance of 6 kpc, with a disk mass of $5 \times 10^{10} M_\odot$ and are otherwise identical to the previous simulations with $\theta = 22.5^\circ$.

The impact of orbital inclination on the mass of the star cluster is shown in Figure 6. We plot the total mass vs. time taking as a reference a simulated star cluster in a “regular” or “standard” orbit with an inclination of $\theta \sim 22.5^\circ$. We also plot the total masses of the simulated star clusters with orbits on the plane of the disk ($\theta = 0$), and perpendicular to it ($\theta = 90^\circ$).

Figure 6 shows that the star cluster in a perpendicular orbit to the plane of the disk is affected by a stronger mass loss than the cluster in a less inclined orbit or the cluster in an orbit in the plane of the disk. The simulated cluster on the orbit perpendicular to the disk is fully dissolved in 12.3 Gyr. After 12 Gyr of evolution, the simulated cluster evolving in the plane of the disk is 87 times more massive than the cluster on the orbit perpendicular to the disk. That is a total mass difference of $4477 M_\odot$.

The models discussed in this section show that the compressive shocks experienced by the star cluster at each disk crossing are a dominant factor driving its dissolution. The variable gravitational potential generated by the presence of the disk on the orbit of the star cluster plays a more important role in the dissolution of the cluster than a constant and higher tidal field experienced by a star cluster that evolves in the plane of the disk. Note that star clusters with a small inclination angle with re-

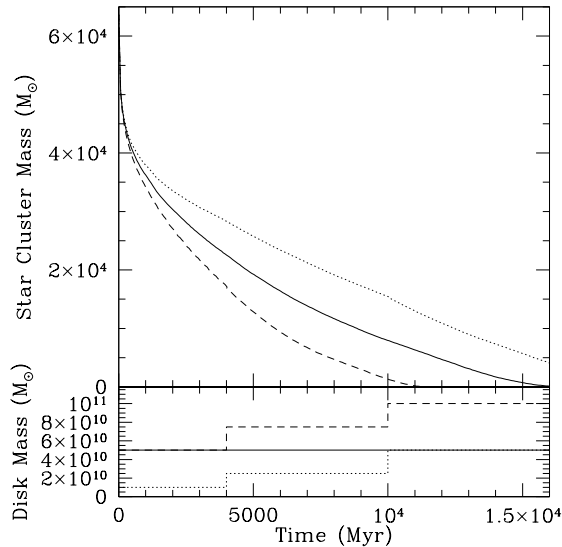


FIG. 7.— Star cluster mass vs. time for different evolution scenarios. The accretion events experienced by the host galaxy can determine the survival or dissolution of a satellite star cluster. The solid line represents the star cluster evolving on a host galaxy with a constant disk mass of $5 \times 10^{10} M_{\odot}$. The lower panel displays the evolution of the disk mass that increases over time with discrete accretion events.

spect to the disk will experience additional shocking due to the presence of spiral arms (Gieles et al. 2007).

7. GALAXY EVOLUTION AND THE SURVIVAL OR DISSOLUTION OF A STAR CLUSTER

At the present time NBODY6 does not allow for a dynamic host galaxy model. However, the first steps to include a time dependent potential have already been taken by Renaud et al. (2011). Within the current framework of NBODY6, and in order to investigate the fate of a star cluster whose host galaxy grows with time, different simulations of star clusters evolving with different disk masses are combined together. These are the simulations presented in Section 3.

Two different pathways for the evolution of a star cluster are built. The first series of accretion events experienced by the host galaxy leads to the survival of the star cluster after a Hubble time. The second scenario, where mass accretion lead to a more massive disk than in the first case, brings the star cluster to a complete dissolution before a Hubble time.

In the first scenario a simulated star cluster evolves during 4 Gyr as the satellite of a host galaxy with a disk mass of $1 \times 10^{10} M_{\odot}$. At 4 Gyr the host galaxy undergoes an instantaneous accretion event that brings the mass of the disk to $2.5 \times 10^{10} M_{\odot}$. At 10 Gyr the host galaxy experiences a second accretion event that brings the host galaxy disk to a mass of $5 \times 10^{10} M_{\odot}$. In this scenario, after a Hubble time, the star cluster has more mass than a simulated star cluster that evolves for a Hubble time in a galaxy with a constant disk mass of $5 \times 10^{10} M_{\odot}$, as expected.

In the second scenario the star cluster begins its evolution in a galaxy with a disk mass of $5 \times 10^{10} M_{\odot}$, at 4 Gyr the disk mass increases to $7.5 \times 10^{10} M_{\odot}$ and at 10 Gyr it increases again to become $10 \times 10^{10} M_{\odot}$. The simulated

star cluster is fully dissolved before a Hubble time due to the enhanced mass loss rates induced by these series of accretion events that built a more massive disk. Note that during this exercise the geometrical parameters of the disk are kept constant $a = 4$ and $b = 0.5$ kpc.

The evolution of the total mass of the star cluster as a function of time in the two scenarios of accretion undergone by the host galaxy described above are given in Figure 7. In addition to these two accreting models the mass evolution of a star cluster evolving around a disk with a constant mass of $5 \times 10^{10} M_{\odot}$ is also plotted. This exercise shows how different accretion histories can lead to different depletion rates of satellite star clusters.

The results of this section can be obtained by joining together the appropriate curves from Fig. 1. For instance, we reconstruct a galaxy evolving in mass above by joining the mass loss rates of a galaxy with a constant disk mass of 1, 2.5, and $5 \times 10^{10} M_{\odot}$ plotted in Fig. 1. The results of this section are also in agreement with Equation 5 on Section 3 that yields a relation between dissolution time, relaxation time, and the disk mass of the host galaxy. This equation shows, for instance, that increasing the disk mass from $1 \times 10^{10} M_{\odot}$ to $10 \times 10^{10} M_{\odot}$ accelerates the destruction time of a star cluster from $56 t_{rh}$ to $11 t_{rh}$.

We should note that we do not claim that the exercise above represents a realistic mass growth history of the Milky Way. Discrete accretion events simulates what is certainly a smoothly growing galaxy. An exciting future perspective is to have upcoming versions of NBODY6 with a fully incorporated time dependent host galaxy potential.

8. FINAL REMARKS

The simulations presented in this work show that star clusters experience first hand the merger and accretion history of their host galaxy. The mass of the host galaxy disk plays an important and measurable role in the evolution of satellite star clusters, by affecting their mass loss rates and thus their structural parameters. The N -body models of star clusters have shown that different masses and geometries of the host galaxy disk can lead to different substructure within the inner 15 kpc of the galactic center. With each galaxy having a different mass growth history, there is still a lot of work to understand how these different histories affect globular clusters. The mass and geometry of the disk affect directly the depletion rates of satellite stellar systems in a similar manner as dark matter halos are affected (D’Onghia et al. 2010).

Assuming a constant disk mass over a Hubble time, as it is often done, can lead to an overestimate of the dissolution rates of globular clusters and thus impact the derived globular cluster mass function.

We would like to thank the referee for a constructive report that helped to improve this paper. This research has made use of the NASA Astrophysics Data System Bibliographic services (ADS) and Google. This work was performed on the gSTAR national facility at Swinburne University of Technology. gSTAR is funded by Swinburne and the Australian Governments Education Investment Fund. Many thanks to Darren Croton, Chris Flynn, Anna Sippel (Swinburne) and Allan Duffy (Mel-

TABLE 2
PARAMETERS OF MODELS EXECUTED

Label	Bulge Mass (M_{\odot})	Disk Mass (M_{\odot})	a (kpc)	b (kpc)	R_{GC} (kpc)	t_{rh} (Gyr)	$t_{10\%}$ (Gyr)
1	1.5×10^{10}	5×10^{10}	0.4	0.5	4	0.1	0.3
2	1.5×10^{10}	5×10^{10}	0.4	0.5	6	1.1	7.2
3	1.5×10^{10}	5×10^{10}	0.4	0.5	8	2.6	—
4	1.5×10^{10}	5×10^{10}	0.4	0.5	10	4.5	—
5	1.5×10^{10}	5×10^{10}	0.4	0.5	12.5	6.6	—
6	1.5×10^{10}	5×10^{10}	0.4	0.5	15	8.6	—
7	6.5×10^{10}	0	—	—	6	8.7	6.1
8	1.5×10^{10}	1.0×10^{10}	4.0	0.5	6	2.6	16.8
9	1.5×10^{10}	2.5×10^{10}	4.0	0.5	6	2.3	15.3
10	1.5×10^{10}	5.0×10^{10}	4.0	0.5	6	1.7	11.0
11	1.5×10^{10}	7.5×10^{10}	4.0	0.5	6	1.2	6.8
12	1.5×10^{10}	10×10^{10}	4.0	0.5	6	0.9	4.8
13	1.5×10^{10}	5×10^{10}	4.0	0.5	4	0.9	5.1
14	1.5×10^{10}	5×10^{10}	4.0	0.5	8	2.8	—
15	1.5×10^{10}	5×10^{10}	4.0	0.5	10	4.0	—
16	1.5×10^{10}	5×10^{10}	4.0	0.5	12.5	5.6	—
17	1.5×10^{10}	5×10^{10}	4.0	0.5	15	7.2	—
18	1.5×10^{10}	5×10^{10}	8.0	0.5	4	1.4	9.2
19	1.5×10^{10}	5×10^{10}	8.0	0.5	6	2.3	14.5
20	1.5×10^{10}	5×10^{10}	8.0	0.5	8	3.1	18.6
21	1.5×10^{10}	5×10^{10}	8.0	0.5	10	3.9	22.8
22	1.5×10^{10}	5×10^{10}	8.0	0.5	12.5	5.0	—
23	1.5×10^{10}	5×10^{10}	8.0	0.5	15	6.3	—

NOTE. — NOTE. — Column 1 gives the model label; Column 2 bulge mass in solar masses; Column 3 disk mass in solar masses; Column 4: Miyamoto disk scale length a ; Column 5 Miyamoto scale height b ; Column 6 Galactocentric distance; Column 7: half-mass relaxation time (t_{rh}); Column 8: time when the star cluster has only 10% of the initial mass left $t_{10\%}$ — Columns 7 and 8 are proxies for the dissolution time.

bourne University) for asking the inquisitive questions that inspired this work.

REFERENCES

- Aarseth, S. J. 1999, *PASP*, 111, 1333
Aarseth, S. J. 2003, *Gravitational N-body Simulations: Tools and Algorithms* (Cambridge Monographs on Mathematical Physics). Cambridge University Press, Cambridge
Aguilar, L., Hut, P. & Ostriker, J. P. 1988, *ApJ*, 335, 720
Binney, J. & Tremaine, S. *Galactic Dynamics*, Princeton University Press, Princeton, New Jersey, 1987, p. 514.
Bullock, J. S. & Johnston, K. V. 2005, *ApJ*, 635, 931
Baumgardt, H. & Makino, J. 2003, *MNRAS*, 340, 227
D’Onghia, E., Springel, V., Hernquist, L., & Keres, D. 2010, *ApJ*, 709, 1138
Gieles, M. et al. 2007, *MNRAS*, 376, 809
Gnedin, O. Y., & Ostriker, J. P. 1997, *ApJ*, 474, 223
Gnedin, O. Y., & Ostriker, J. P. 1999, *ApJ*, 513, 626
Gómez, F. A., Helmi, A., Brown, A. G., & Li, Y-S. 2010, *MNRAS*, 408, 935
Kroupa, P., Tout, C. A., Gilmore, G. 1993, *MNRAS*, 262, 545
Kroupa, P. 2001, *MNRAS*, 322, 231
Kundic, T. & Ostriker, J. P. 1995, *ApJ*, 438, 702
Küpper, A. H., Kroupa, P., Baumgardt, H., Heggge, D. C. 2010, *MNRAS*, 401, 105
Leitner, S. N. 2012, *ApJ*, 745, 149
Madrid, J. P., Hurley, J. R., Sippel, A. C. 2012, *ApJ*, 756, 167
Miyamoto, M. & Nagai, R. 1975, *PASJ*, 27, 533
Odenkirchen, M. et al. 2001, *ApJ*, 548, L165
Paczynski, B. 1990, *ApJ*, 348, 485
Peñarrubia, J., Belokorov, V., Evans, N. W., et al. 2010, *MNRAS*, 408, L26
Portegies Zwart, S. F., McMillanm S. L. W., Gieles, M. 2010, *ARA&A*, 48, 431
Plummer, H. C. 1911, *MNRAS*, 71, 460
Renaud, F., Gieles, M., & Boily, C. M. 2011, *MNRAS*, 418, 759
Renaud, F. & Gieles, M. 2013, *MNRAS*, 431, L83
Spergel, D. N., et al. 2003, *ApJSS*, 148, 175
Spitzer, L. 1958, *ApJ*, 127, 17
Spitzer, L. & Hart, M. H. 1971, *ApJ*, 164, 399
Read, J. I., Wilkinson, M. I., Evans, N., Gilmore, G., & Kleyna, J. T. 2006, *MNRAS*, 367, 387
Renaud, F., Gieles, M. & Boily, C. M. 2011, *MNRAS*, 418, 759
Vesperini, E. & Heggge, D. C. 1997, *MNRAS*, 289, 898
West, M. J., Côté, P., Marzske, R. O., Jordán, A. 2004, *Nature*, 427, 31
White, S. D. M. & Rees, M. J. 1978, *MNRAS*, 183, 341
Xue, X. X., et al. 2008, *ApJ*, 684, 1143